



The Paleoclimate Significance of the $\delta^{13}\text{C}$ Composition of Individual Hydrocarbon Compounds in the Maoming Oil Shales, China

Xinxing Cao^{1,2}, Zhiguang Song^{1*}, Sib0 Wang¹ and Puliang Lyu²

¹ Faculty of Chemical and Environmental Sciences, Guangdong Ocean University, Zhanjiang, China, ² Key Laboratory of Beibu Gulf Environmental Change and Resources Utilization of Ministry of Education, Nanning Normal University, Nanning, China

OPEN ACCESS

Edited by:

Francesco Italiano,
National Institute of Geophysics
and Volcanology, Section of Palermo,
Italy

Reviewed by:

Dazhen Tang,
China University of Geosciences,
China
Yongli Wang,
Chinese Academy of Sciences, China

*Correspondence:

Zhiguang Song
zsong@gig.ac.cn

Specialty section:

This article was submitted to
Geochemistry,
a section of the journal
Frontiers in Earth Science

Received: 31 December 2020

Accepted: 02 March 2021

Published: 29 March 2021

Citation:

Cao X, Song Z, Wang S and Lyu P
(2021) The Paleoclimate Significance
of the $\delta^{13}\text{C}$ Composition of Individual
Hydrocarbon Compounds
in the Maoming Oil Shales, China.
Front. Earth Sci. 9:648176.
doi: 10.3389/feart.2021.648176

Maoming oil shales are typical low-altitude lacustrine sediments that were deposited during the late Paleogene. The hydrocarbon composition and compound-specific stable carbon isotopic composition ($\delta^{13}\text{C}$) of organic matter in the profile samples of the oil shales have been analyzed. The results show that algae and aquatic plants are major parent sources of the organic matter in the oil shales associated with a small portion of terrestrial higher plant input. The $\delta^{13}\text{C}$ composition of the bulk organic matter and the *n*-alkanes varies greatly on the profile from -26.9 to -15.8‰ and -31.7 to -16.2‰ , respectively. While a good positive correlation among the $\delta^{13}\text{C}$ composition of individual *n*-alkanes implies that these *n*-alkanes were originated from the similar source input. The $\delta^{13}\text{C}$ composition of *n*-alkanes on the profile displays a positive excursion trend from the bottom to the top, and this excursion was likely related to the general decreasing trend of the partial pressure of atmospheric CO_2 ($p\text{CO}_2$) during the late Paleogene. The $\delta^{13}\text{C}$ composition of the C_{30} -4-methyl steranes ranges from -11.9 to -6.3‰ , which is suggestive of *Dinoflagellates*-related source input. Coincidentally, the high abundance C_{33} -botryococcanes were detected in the samples on the top section of the profile and display an extremely positive carbon isotopic composition of -4.5 to -8.4‰ , suggesting that the lower partial pressure of atmospheric CO_2 had triggered a bicarbonate consumption mechanism for *Botryococcus braunii* B. Therefore, the $\delta^{13}\text{C}$ composition of *n*-alkanes and C_{33} -botryococcanes and their profile variation suggest that a general declining process associated with fluctuation in the partial pressure of atmospheric CO_2 is likely the major reason for the rapid climatic changes toward the end of the late Paleogene.

Keywords: *n*-alkanes, botryococcane, $\delta^{13}\text{C}$ of individual compounds, Maoming oil shales, the late Paleogene

HIGHLIGHTS

- The algae and macrophyte are major source inputs of organic matter in Maoming oil shales.
- The biomarker ratios indicate oxidized condition for early stage of oil shale deposition.
- The $\delta^{13}\text{C}$ of source specific biomarkers suggest carbon source shift for specific algae.
- An upward positive excursion of the $\delta^{13}\text{C}$ of *n*-alkanes implies a decreasing atmospheric $p\text{CO}_2$.

INTRODUCTION

The paleoclimate had experienced rapidly significant variation during the late Paleogene, as the global climate was switched from the warm “greenhouse” into the “glaciation and interglacial periods” from the Eocene to the Oligocene (Liu et al., 2009; Pearson et al., 2009; Colwyn and Hren, 2019). The evidence of these significant climate changes including the fast formation of the Antarctic ice sheet, the carbonate compensation depth (CCD) rapid deepened and the increase of the oxygen isotope ratio ($\delta^{18}\text{O}$) of deep-sea benthic foraminifera (Tripathi et al., 2005; Liu et al., 2009; Galeotti et al., 2016; McKay et al., 2016; Passchier et al., 2017). However, the process and the reason for climate change are not well understood yet. The most of previous studies based on marine sediments suggested that the climate change would be connected with the decline of atmospheric carbon dioxide (CO_2) concentration, the switch of ocean current system and the variation of the solar radiation (Coxall et al., 2005; Goldner et al., 2014; Liu et al., 2018; Gallagher et al., 2020). On the other hand, some studies of lacustrine records are not well consistent with marine records and suggested that there was a significant climate cooling with obviously seasonal climate change, and the regional aridification in the middle and high latitude continental areas, while some other studies suggested minor or insignificant climate changes (Stephen et al., 2005; Dupont-Nivet et al., 2007; Pei et al., 2007; Eldrett et al., 2009; Hren et al., 2013; Fang et al., 2019; Ao et al., 2020). Obviously, the systematic research on more terrigenous records, especially the records of the low latitude lacustrine sediments, is much needed to the full understanding of the climate change in the late Paleogene.

The Maoming oil shales are typical low-latitude lacustrine organic-rich sediments. According to the age dating based on the turtle fossils and sporopollen (Chow, 1956; Chow and Yeh, 1962), the Maoming oil shales were widely considered as deposited during the late Eocene to early Oligocene, while a few researchers suggested that the oil shales were deposited in the early and middle Oligocene or the late Eocene (Yu and Wu, 1983; Jin, 2008; Li Y.X. et al., 2016). Therefore, the detailed geochemical research on the Maoming oil shales could provide significant information on the regional paleoclimate change of the late Paleogene in the low-latitude continental region. Previous studies have mainly focused on the source inputs and hydrocarbon composition and distribution of organic matter in Maoming oil shales (Brassell et al., 1986; Meng et al., 2020). For example, Yu et al. (2000) suggested the multi-source inputs of organic matter in Maoming oil shales based on $\delta^{13}\text{C}$ of *n*-alkanes in one outcrop sample, while others had analyzed the hydrocarbon compounds and identified a number of the biomarkers such as botryococcanes, 4-methyl steranes and hopanes in some oil shale samples (Fu et al., 1985; Brassell et al., 1986; Liao et al., 2018). Although these researches have provided some useful information on characterizing organic matter in the Maoming oil shales, all these studies are carried out on the casual outcrop samples and there is a lack of the systematic research on the characteristics of organic matter in the oil shales of the whole profile.

Therefore, by studying the composition and distribution of hydrocarbon compounds including biomarkers and their $\delta^{13}\text{C}$ composition and profile variations in the oil shale samples symmetrically collected from a full drill core from Maoming Basin, this study aims to correlate organic geochemical profile of the oil shales with the paleoenvironment variation during the geological period of the Maoming oil shale sedimentation, and therefore to provide better understanding of the climate changes of low-latitude continent region during the late Palaeogene.

GEOLOGICAL SETTING AND SAMPLES

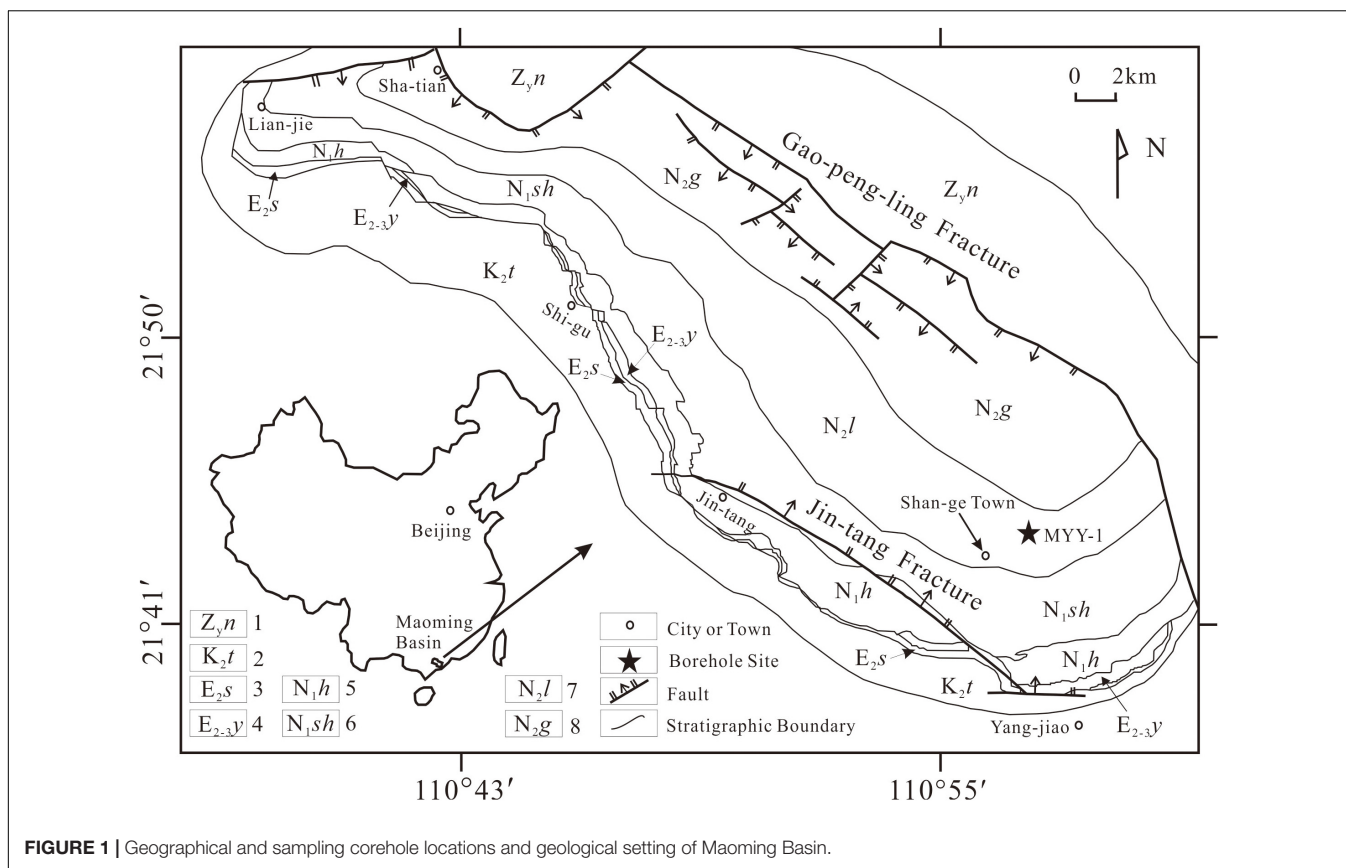
The Maoming oil shales are named after the Maoming Basin, which is located in Southwest Guangdong province, China. The geographical and sampling corehole locations associated with geological settings are presented in **Figure 1**. The sediments of Maoming Basin were stratigraphically divided into Tongguling Formation, Shangdong Formation, Youganwo Formation, Huangniuling Formation, Shangcun Formation, Laohuling Formation and Gaopengling Formation from the bottom to the top (Herman et al., 2017). The Youganwo Formation is mainly comprised of organic-rich oil shales with a thickness varying from 2 to 45.5 m and was widely regarded as deposited from the late Eocene to the early Oligocene. The detailed lithology of Youganwo Formation includes brown tight laminar oil shales interlayered with thin clay beds, fine sandstones, carbonaceous shales, lignite, biological debris argillaceous limestone and volcanic tuff (Brassell et al., 1986; Bureau of Geology and Mineral Resources of Guangdong Province, 1996).

The core samples of Maoming oil shales were collected from the “MY-1” borehole, which is located at Shan-ge Town of the Southwestern Maoming Basin (N21°44′20″, E110°57′29″). The drilling depth of the “MY-1” borehole is 860 m and the Youganwo Formation covers the depth from 811 to 857 m, while the depth of the oil shales is from 815 to 854.3 m. The top section of the Youganwo Formation on this borehole is comprised of fine sandstone and carbonaceous shales burying at the depth of 811 to 815 m. And the bottom section of Youganwo Formation is consisted of some lignite layers and some carbonaceous shale layers at the depth of the 854.3 to 857 m. A total of 37 oil shale samples were selected from the core profile at a consistent interval (**Table 1**).

EXPERIMENTAL PROCEDURES

The total organic carbon content (TOC) and pyrolysis data of the core samples was determined using the Rock-Eval 6 pyrolyzer manufactured by French Vinci Technologies (**Table 1** and **Figure 2**), with measurement error of 0.05% for the total organic carbon content (TOC). The sample preparation was to take about 20 mg of oil shale samples and put into a ceramic crucible and then covered up with quartz sand, the sample crucibles were baked at 850°C for 2 h before the pyrolysis measurement.

For soluble organic matter extraction, the oil shale samples were ground to less than 100 meshes and then solvent extracted



using Soxhlet-extractor for 72 h. The extracts of soluble organic matter were separated into asphaltene fraction, aliphatic fraction, aromatic fractions and polar compounds, while the aliphatic fraction was further separated into *n*-alkane and branched and cyclic alkane fractions. The detailed experimental procedures and methods can be found in the reference of Li Y. et al. (2016). The aliphatic fractions were subjected to the analysis of the gas chromatograph (GC) and the gas chromatograph-mass spectrometry (GC-MS). The *n*-alkane and branched and cyclic alkane fractions were further analyzed by the GC-MS and the gas chromatograph-isotope ratio mass spectrometry (GC-IRMS).

The gas chromatographic analysis was carried out on an Agilent 7890A GC coupled with a flame ionization detector and the GC-MS was performed using Thermo GC Ultra Trace-DSQ II MS with an electron impact ion source at 70 eV. The capillary column used in GC and GC-MS were a J&W DB-5 fused silica column (30 m × 0.25 mm i.d. × 0.25 μm film thickness), with the injector and detector temperatures were 290 and 300°C, respectively. The samples were injected in splitless mode, and N₂ and helium are the carrier gases for GC and GC-MS, respectively. The oven temperature was initially set at 80°C and held for 2 min, was programmed to 130°C at a rate of 20°C/min, then was programmed to 290°C at 3°C/min and held for 20 min.

The carbon isotopic composition analyses of *n*-alkanes and branched and cyclic (b & c) alkanes were carried out on an Isoprime GC-Isotope Ratio Mass Spectrometer (GC-IRMS). The alkane samples were injected in splitless mode, and the injector

temperature was set at 290°C with helium as the carrier gas. A J&W DB-5 silica capillary column (30 m × 0.25 mm i.d. × 0.25 μm film thickness) was used for the separation elution of *n*-alkane and branched and cyclic alkane compounds. The oven temperature was initially set at 80°C and held for 2 min, and programmed to 130°C at a rate of 20°C/min, and then increased to 290°C at 3°C/min heating rate and held for 20 min. The b & c alkanes were identified based on the retention time of GC-MS chromatograms. The $\delta^{13}\text{C}$ composition of all samples was measured at least twice and the average $\delta^{13}\text{C}$ values of the individual compounds are reported here. The GC-IRMS was calibrated using the Vienna Peedee Belemnite (VPDB) standard and the isotopic measurement error of parallel analyses was <0.5‰. A standard sample of mixed *n*-alkanes (*n*-C₁₂ ~ *n*-C₃₂) with known isotopic composition was also measured daily to ensure the reliability of the instrument.

RESULTS AND DISCUSSION

General Characteristics of Organic Matter in Maoming Oil Shales

The total organic carbon content (TOC) of Maoming oil shales ranges from 5.1 to 28.9% (Table 1), and the TOC contents in most samples are close to or greater than 10%, except these carbonaceous shale samples from the bottom of the Youganwo Formation. The TOC content also shows significant variation

TABLE 1 | Sampling information and the pyrolytical data of Maoming oil shales.

Sample name	Borehole depth (m)	TOC (%)	Tmax (°C)	S ₁ (mg/g)	S ₂ (mg/g)	S ₃ (mg/g)	HI (mg/gTOC)	OI (mg/gTOC)
MY-3	815.0	11.1	435	0.88	84.72	0.84	763	8
MY-4	816.0	9.9	431	0.67	71.06	5.5	716	55
MY-6	817.3	19.1	432	1.89	164.1	6.2	857	32
MY-7	817.8	13.1	433	1.32	104.44	2.79	795	21
MY-8	818.4	13.3	434	0.64	95.97	0.9	719	7
MY-10	819.6	11.4	434	0.58	91.24	5.18	800	45
MY-12	821.0	16.4	435	1.28	128.91	1.19	785	7
MY-13	821.8	11.6	433	0.76	93.47	3.93	808	34
MY-14	822.3	9.7	430	0.6	74.28	0.83	767	9
MY-17	824.6	10.7	434	0.44	81.58	0.68	760	6
MY-20	826.2	9.9	429	0.69	75.57	5.58	764	56
MY-22	827.5	14.0	434	0.74	115.31	1.16	825	8
MY-23	828.8	16.4	437	0.65	128.4	2.79	784	17
MY-24	829.6	13.7	431	0.83	109.82	1.05	804	8
MY-25	830.4	10.5	433	0.64	82.49	1.13	783	11
MY-26	830.8	12.8	435	0.53	100.75	0.8	789	6
MY-27	831.4	18.0	431	1.61	154.6	2.17	860	12
MY-28	832.0	9.2	434	0.38	71.69	0.38	777	4
MY-29	832.5	13.8	434	0.79	121.7	1.62	882	12
MY-31	833.7	13.1	434	0.7	101.29	0.71	771	5
MY-32	834.5	16.3	435	1.45	146.62	5.2	900	32
MY-33	835.0	12.1	432	0.62	88.63	0.59	730	5
MY-34	835.8	17.5	435	1.67	210.82	1.84	901	8
MY-35	836.5	15.3	432	0.38	110.83	1.07	725	7
MY-36	837.5	14.3	433	1.01	122.68	1.57	857	11
MY-37	838.8	12.0	431	0.69	93.79	0.66	782	6
MY-40	840.2	16.3	434	1.04	124.28	0.95	764	6
MY-43	841.5	13.5	431	0.95	97.19	4.65	719	34
MY-45	842.7	28.9	436	1.8	234.79	1.72	813	6
MY-47	844.2	10.3	425	0.68	58.78	6.01	573	59
MY-50	845.8	26.7	437	1.3	214.94	1.48	806	6
MY-53	847.8	13.6	425	1.46	97.56	5.23	717	38
MY-55	849.0	22.2	429	1.75	167.19	1.48	754	7
MY-57	850.0	15.3	427	1.44	96.14	7.74	628	51
MY-59	850.9	20.0	430	1.85	153.93	1.42	768	7
MY-62	852.7	9.0	427	0.33	53.97	0.66	598	7
MY-64	853.9	5.1	427	0.36	19.99	3.25	391	64

Hydrogen Indices (HI) are calculated from the ratio of mg HC in S₂/g TOC, and Oxygen Indices (OI) are determined by the ratio of mgCO₂ in S₃/g TOC.

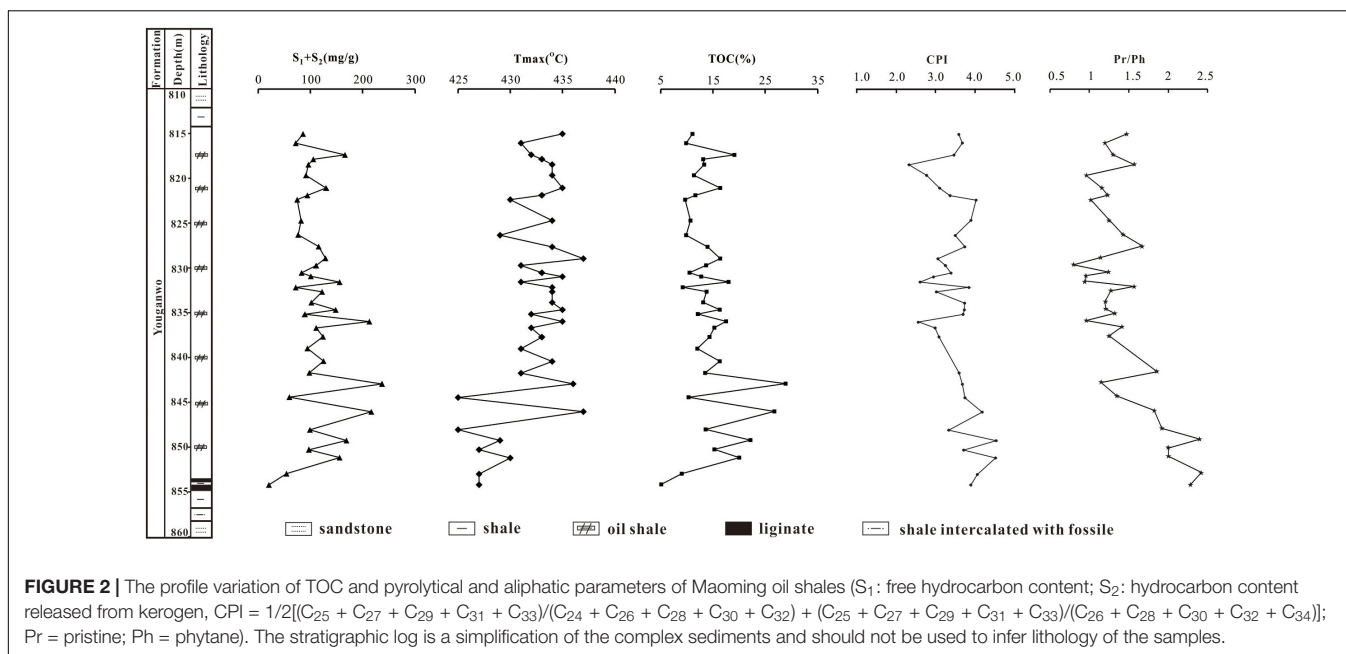
in different section of the profile, as the TOC content of the lower section oil shales on the profile from 840 to 852 m is in the range of 10.3 to 28.9% (with an average of 18.5%), while the TOC content of the upper section oil shales on the profile from 815 to 840 m vary from 9.2 to 19.1% (with an average of 13.3%). Obviously, the organic matter abundance in the lower section oil shales is higher than that of the upper section oil shales on the profile.

The thermal pyrolysis data suggested that these Maoming oil shales are thermally immature or low mature (Peters and Cassa, 1994), as their T_{max} values range from 425 to 437°C and most of them were under 435°C (Table 1 and Figure 2). The free hydrocarbon content (S₁) ranges from 0.33 to 1.89 mg/g (with average of 0.96 mg/g), indicating a high variability of liquid hydrocarbon contents in these shales, and the hydrocarbon

content released from the thermal crack of kerogen (S₂) vary from 19.99 to 234.79 mg/g (with an average of 111.99 mg/g). The hydrogen index (HI) and oxygen index (OI) values of Maoming oil shales are in the range of 391–901 mg/gTOC and 4–64 mg/gTOC, respectively (Table 1). The S₁ + S₂ values varied from 20.35 to 236.59 mg/g (with an average of 112.94 mg/g), and most of them were around 100 mg/g, which illustrate high hydrocarbon generation potential of Maoming oil shales.

The Composition and Distribution of Aliphatic Hydrocarbon Compounds

The composition and distribution of aliphatic hydrocarbon compounds in Maoming oil shales include a series of compounds such as *n*-alkanes, branched and acyclic isoprenoids, hopanes



and steranes, with *n*-alkanes are the dominant components. The chromatograms of aliphatic fraction in representative oil shale samples are displayed in **Figure 3**. The carbon number of the *n*-alkanes is principally distributed in the range of *n*-C₁₃ to *n*-C₃₃, while these normal alkanes display a clear bimodal distribution with clear rear peak group dominance as the *n*-C₂₇ being the predominance *n*-alkane peak on the chromatograms of all samples on the profile. The front peak group of low carbon number alkanes is dominated by *n*-C₁₇ or *n*-C₁₅, while the rear peak group of high carbon number *n*-alkanes is solely dominated by *n*-C₂₇. The high carbon number *n*-alkanes display obviously a carbon number predominance of odd-over-even, as the carbon-preference index (CPI) of *n*-C₂₄ to *n*-C₃₄ is in the range of 2.33 to 4.54 on the whole profile (**Figure 2**), indicating low maturity or immaturity. Although the overall dominance of rear peak group over the front peak group of *n*-alkanes, the relative abundance of front peak group *vs.* the rear peak group show some variation along with burying depth on the profile, and these variation are likely due to the slightly change in the source inputs of organic matter. The relative abundance of low and medium carbon number alkanes of *n*-C₁₃ to *n*-C₂₁ and *n*-C₂₂ to *n*-C₂₆ varies along with bearing depth and the whole profile could be divided into three sections according to the distribution of the *n*-alkanes. The section I ranging from 815 to 828 m and the section III ranging from 840 to 854 m are characterized by relative lower abundance of low and medium carbon number *n*-alkanes, while the section II ranging from 828 to 840 m are characterized by relative higher abundance of low and medium carbon number *n*-alkanes.

Generally, the low carbon number *n*-alkanes (carbon number $\leq n$ -C₁₉) are considered as originated from algae and photosynthetic bacteria inputs (Gelpi et al., 1970; Meyers, 2003; Kristen et al., 2010), the medium-chain *n*-alkanes (*n*-C₂₀ ~ *n*-C₂₆) often indicate aquatic plant sources (Ficken et al., 2000;

Mügler et al., 2008; Aichner et al., 2010; Damsté et al., 2011), while the high carbon number *n*-alkanes (carbon number $\geq n$ -C₂₇) with an odd-over-even predominance are widely considered as related with terrestrial higher plant inputs (Eglinton and Hamilton, 1967). Therefore, some samples in section II (for example, MYY-24 at 829.6 m depth) contain high abundance of the medium carbon number *n*-alkanes, which suggested an incremental input of algae and macrophyte (Gelpi et al., 1970).

The main acyclic isoprenoids include the pristane (Pr) and the phytane (Ph) which occur in high abundance in all samples of whole profile. The Pr/Ph ratio (**Figure 2**) vary in the range of 0.80 to 2.42 on the profile and displays profile variation as it is in the range of 0.80 to 1.67 for section I and section II, and 1.15 to 2.42 for section III, respectively. Since the Pr/Ph ratio between 0.80 and 3.5 could not be solely used as depositional redox indicator, the Pr/Ph ratios of these oil shales should be combined with other proxies to reconstruct the paleoenvironment variation.

The Composition and Distribution of Biomarkers

A great number of biomarkers including steroid and hopane compounds are detected in all the oil shale samples (**Figures 4, 5**).

The steranes identified in Maoming oil shales are mainly included the regular steranes, rearranged steranes (diasteranes), 4-methyl steranes and 4-methyl rearranged steranes (4-methyl diasteranes). The sedimentary steranes are often transformed from steroids and sterenes that originated from organisms. The composition and distribution of regular steranes (including C₂₇, C₂₈, C₂₉ steranes) are consistent in most samples of the whole profile, with the high abundance of C₂₇-cholestanes and C₂₉-cholestanes and the low abundance of C₂₈-cholestanes. The 4-methyl steranes are consisted of a high abundance of the C₃₀-4-methyl steranes, low abundance of C₂₉-4-methyl steranes

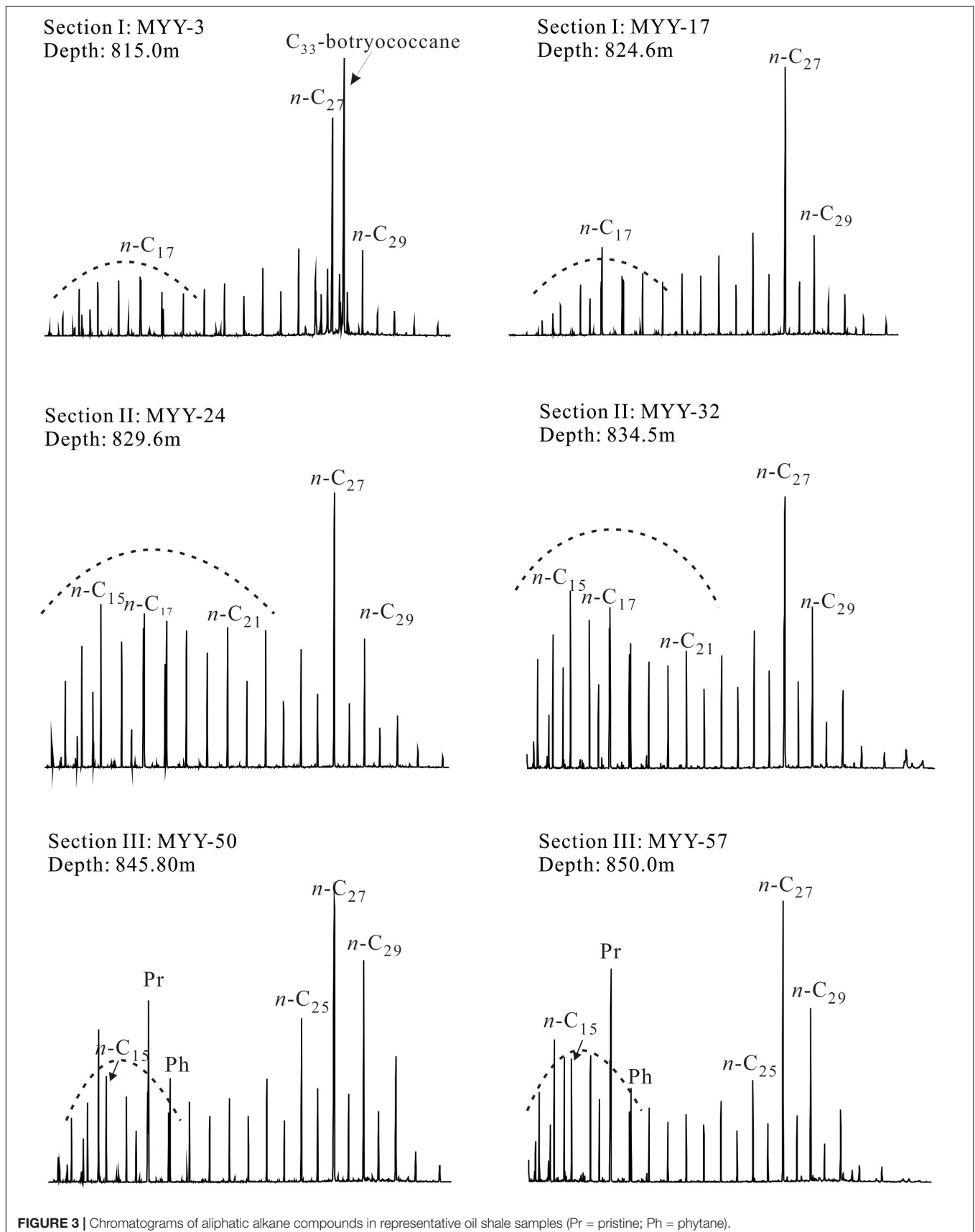


FIGURE 3 | Chromatograms of aliphatic alkane compounds in representative oil shale samples (Pr = pristane; Ph = phytane).

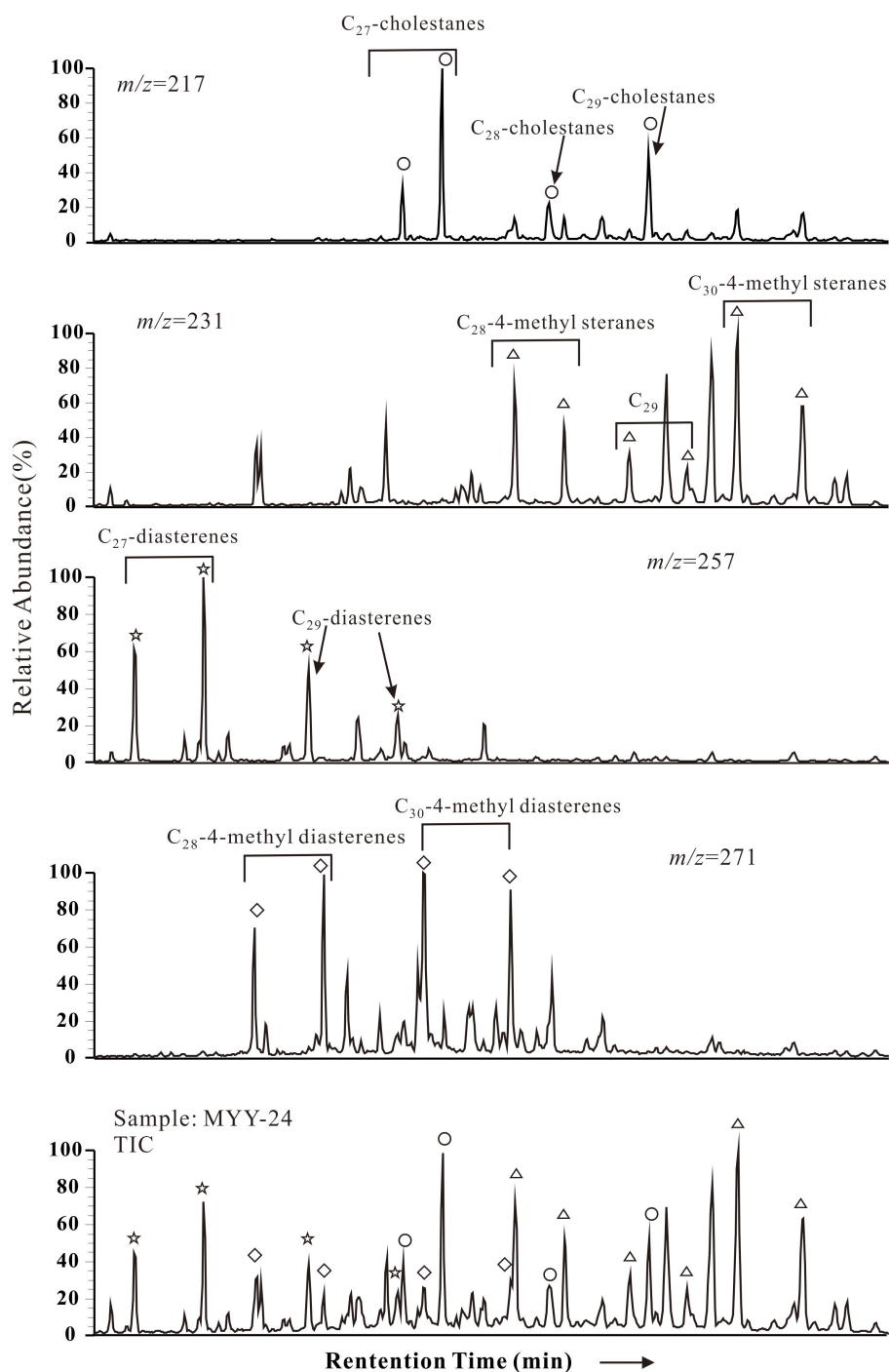


FIGURE 4 | The identification and distribution of steranes in a representative oil shale sample (Note: \circ : regular steranes; Δ : 4-methyl steranes; \star : diasterenes; \diamond : 4-methyl diasterenes; TIC: total ion chromatogram).

and C_{28} -4-methyl steranes. The rearranged steranes are mainly consisted of trace amounts of C_{28} -rearranged steranes, high abundance of the C_{27} -rearranged steranes and C_{29} -rearranged steranes. The 4-methyl rearranged steranes are dominated by a high abundance of the C_{30} -4-methyl rearranged steranes and a relative high amount of C_{28} -4-methyl rearranged steranes, while

the C_{29} -4-methyl rearranged steranes are only detected in trace amount of few samples (Figure 4).

The hopanes are widely present in high abundance in all samples of the whole profile. The main compounds of hopanes are trisnorhopanes, norhopanes, hopanes, homohopanes, $\Delta^{17(21)}$ -hopanes, and $\Delta^{13(18)}$ -neohopanes, but the gammacerane

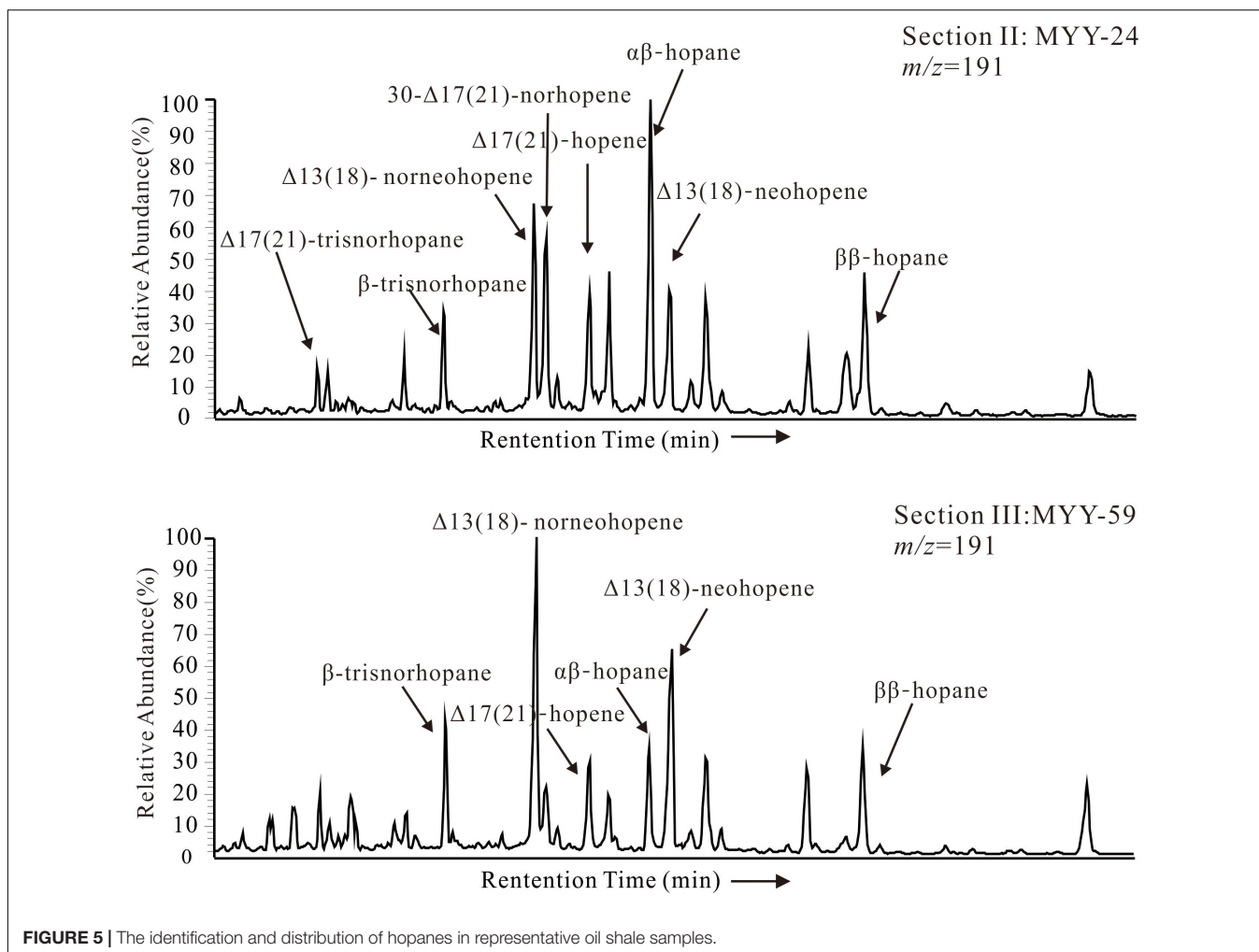


FIGURE 5 | The identification and distribution of hopanes in representative oil shale samples.

is not detected (Figure 5). The hopanes are dominant compounds of pentacyclic-terpane as there are abundant of the $\Delta^{17(21)}$ -hopenes are detected, which are considered as medium products which the $\beta\beta$ -hopanes transformed to $\beta\alpha$ -hopanes and $\alpha\beta$ -hopanes (Zhou et al., 1998). The occurrence of high abundance of $\beta\beta$ -hopanes, $\Delta^{17(21)}$ -hopenes and $\Delta^{13(18)}$ -neohopenes in the samples also indicate that these oil shales of Youganwo Formation are of low maturity.

The composition and distribution of the hopanes and the hopenes in these oil shales are generally similar on the whole profile. However, the abundance of the $\Delta^{17(21)}$ -hopene compounds are very low as the 30- $\Delta^{17(21)}$ -norhopenes and $\Delta^{17(21)}$ -trisorhopenes are absent in section III. On the other hand, the abundance of the $\Delta^{13(18)}$ -neohopene and $\Delta^{13(18)}$ -norneohopene compounds appear to be significantly increased on the section III. Some previous studies suggested that the $\Delta^{13(18)}$ -neohopene is generated from the parent material through molecular bond broke during the late diagenesis; and the others considered that the $\Delta^{13(18)}$ -neohopene was transformed from thermodynamically unstable $\Delta^{17(21)}$ -hopene as suggested by the $\delta^{13}\text{C}$ composition of the hopenes in the peat samples (Zhou et al., 1998).

Since the maturity of oil shale samples show little change on the profile (Figure 2), the lower abundance $\Delta^{17(21)}$ -hopene and the higher abundance for both $\Delta^{13(18)}$ -norneohopene and $\Delta^{13(18)}$ -neohopene in section III than section II might not be related with the diagenesis process, but may be related to the variation in the sedimentary condition. As we have discussed above, the Pr/Ph ratio (Figure 2) shows an increasing trend along with the buried depth in section III, this may suggest that the deposition condition of section III could be more oxidized than that of upper sections. Therefore, the $\Delta^{13(18)}$ -neohopene would be better preserved or formed than $\Delta^{17(21)}$ -hopene under an oxidizing sedimentary condition.

It is worthwhile to point out that C_{33} -botryococcanes and C_{31} -botryococcanes are source-specific biomarkers and has been intermittently detected in high abundance in most samples of the top section at a depth from 815 to 821 m (Figures 3, 6), as the peak height of one C_{33} -botryococcan compound is even higher than that of the dominant *n*-alkane compound of *n*- C_{27} . The botryococcanes are a kind of irregular acyclic isoprenoids and are considered as transformed from botryococcanes, which originated from *Botryococcus braunii* which is a kind of algae living in fresh to brackish water or even estuarine area

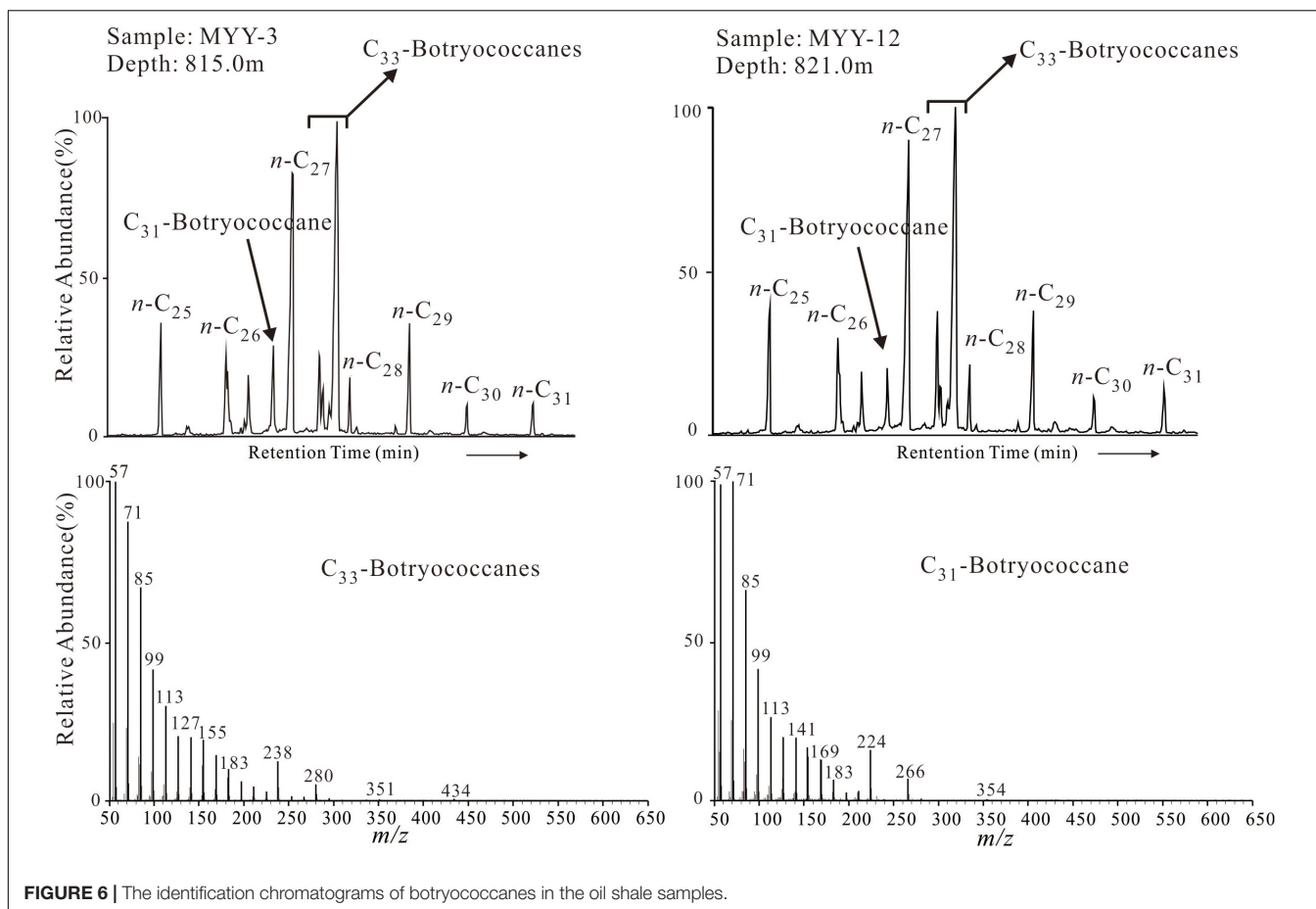


FIGURE 6 | The identification chromatograms of botryococcanes in the oil shale samples.

(Moldowan and Seifert, 1980; McKirdy et al., 1986; Smittenberg et al., 2005; Volkman, 2014). Since the *Botryococcus braunii* is sensitive to the variation of the water condition, the occurrence of botryococcanes in the sediments suggests obvious change in the environmental condition and a decline in the abundance of botryococcanes are often considered as indication of earlier anoxic condition (Smittenberg et al., 2005). The intermittently high abundance presence of the botryococcanes on the top section of the profile indicates that the lake environment was frequently favorable for the thriving of *Botryococcus braunii* B. and therefore there is a significant fluctuation in lake environment during the later stage of sedimentation in the Maoming basin.

The $\delta^{13}\text{C}$ Composition of *n*-Alkanes and Individual Biomarkers

The $\delta^{13}\text{C}$ composition of *n*-alkanes in representative samples of oil shales varies from -31.7 to -16.2‰ on the profile. The $\delta^{13}\text{C}$ composition of *n*-C₁₇ and *n*-C₁₉, which are considered as derived from bacteria and algae, range from -26.9 to -19.6‰ and -29.6 to -20.0‰ , respectively. The $\delta^{13}\text{C}$ of *n*-C₂₃ and *n*-C₂₅, which are often considered as originated mainly from aquatic macrophytes (Ficken et al., 2000), range from -30.2 to -18.4‰ and -29.5 to -18.5‰ , respectively. While the $\delta^{13}\text{C}$ of

these *n*-C₂₇, *n*-C₂₉, *n*-C₃₁, and *n*-C₃₃, that are considered as a predominantly contribution from terrigenous plants, range from -28.8 to -16.2‰ , -28.9 to -20.5‰ , -30.9 to -21.1‰ , and -31.7 to -20.1‰ , respectively. The $\delta^{13}\text{C}$ composition of the same *n*-alkane compounds varies among these samples on the profile (Figure 7).

The profile variation trends of the $\delta^{13}\text{C}$ composition of the medium odd carbon number *n*-alkanes of *n*-C₂₃ and *n*-C₂₅ are similar to that of the high odd carbon number *n*-alkanes of *n*-C₂₇, *n*-C₂₉, and *n*-C₃₁. These shows that the $\delta^{13}\text{C}$ composition variation of individual hydrocarbon compounds are covariant on the profile and therefore suggests that these changes were caused by similar factors, such as changes in organic matter inputs (the direct carbon source) or of partial pressure ($p\text{CO}_2$) of atmospheric CO₂ (the indirect and the elementary carbon source).

The $\delta^{13}\text{C}$ variation trends of individual hydrocarbon compounds are also similar to that of bulk organic matter ($\delta^{13}\text{C}_{\text{org}}$) in the profile (Figure 7). The coefficient of the $\delta^{13}\text{C}$ composition among individual *n*-alkane compounds are analyzed by Pearson correlation methods (level of significance $\alpha = 0.050$). The results show that the $\delta^{13}\text{C}$ of *n*-C₁₇ has low correlation coefficients with that of *n*-C₂₉ (0.388), *n*-C₃₁ (0.440), and *n*-C₃₃ (0.514), while the $\delta^{13}\text{C}$ of *n*-C₁₉ also shows low correlation coefficients with that of *n*-C₂₉ (0.496), *n*-C₃₁

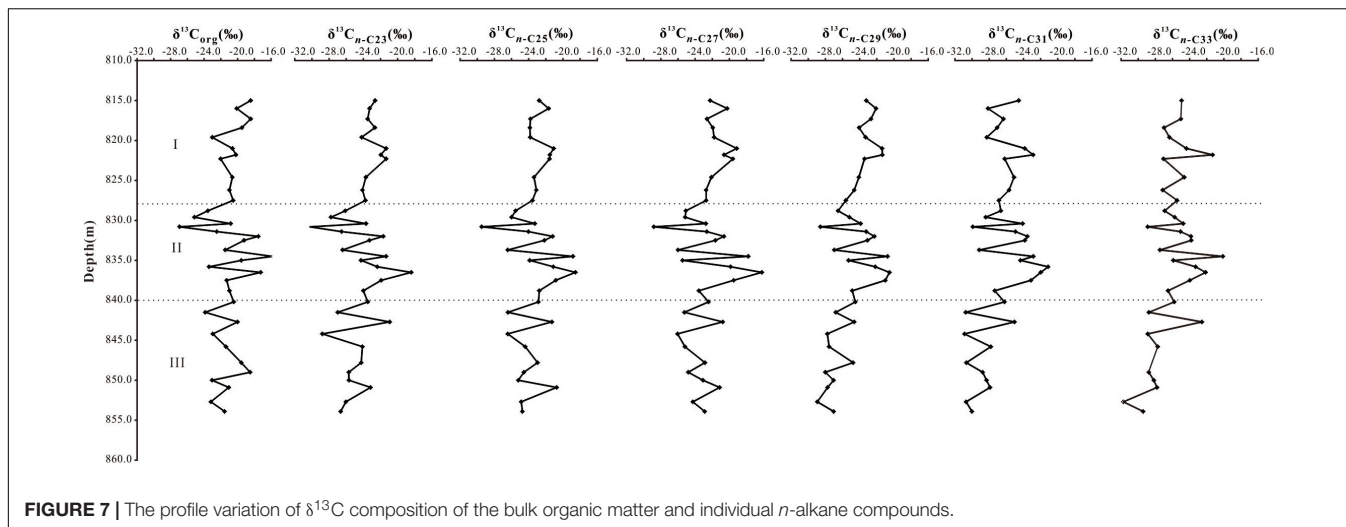


FIGURE 7 | The profile variation of $\delta^{13}\text{C}$ composition of the bulk organic matter and individual n -alkane compounds.

TABLE 2 | Pearson coefficient of correlation between the $\delta^{13}\text{C}$ composition of the bulk organic matter and individual n -alkane compounds.

	$\delta^{13}\text{C}_{\text{org}}$	$\delta^{13}\text{C}_{n-C17}$	$\delta^{13}\text{C}_{n-C19}$	$\delta^{13}\text{C}_{n-C23}$	$\delta^{13}\text{C}_{n-C25}$	$\delta^{13}\text{C}_{n-C27}$	$\delta^{13}\text{C}_{n-C29}$	$\delta^{13}\text{C}_{n-C31}$	$\delta^{13}\text{C}_{n-C33}$
$\delta^{13}\text{C}_{\text{org}}$	1	0.481	0.728	0.714	0.701	0.591	0.532	0.488	0.565
$\delta^{13}\text{C}_{n-C17}$	0.481	1	0.859	0.736	0.694	0.615	0.388	0.440	0.514
$\delta^{13}\text{C}_{n-C19}$	0.728	0.859	1	0.881	0.838	0.731	0.496	0.551	0.531
$\delta^{13}\text{C}_{n-C23}$	0.714	0.736	0.881	1	0.929	0.892	0.758	0.746	0.712
$\delta^{13}\text{C}_{n-C25}$	0.701	0.694	0.838	0.929	1	0.940	0.765	0.731	0.733
$\delta^{13}\text{C}_{n-C27}$	0.591	0.615	0.731	0.892	0.940	1	0.820	0.692	0.707
$\delta^{13}\text{C}_{n-C29}$	0.532	0.388	0.496	0.758	0.765	0.820	1	0.800	0.874
$\delta^{13}\text{C}_{n-C31}$	0.488	0.440	0.551	0.746	0.731	0.692	0.800	1	0.886
$\delta^{13}\text{C}_{n-C33}$	0.565	0.514	0.531	0.712	0.733	0.707	0.874	0.886	1

(0.551), and n -C₃₃ (0.531), respectively. On the other hand, the $\delta^{13}\text{C}$ of n -C₁₉ are closely correlated with the $\delta^{13}\text{C}$ of bulk organic matter, while the $\delta^{13}\text{C}$ of n -C₂₃, n -C₂₅, and n -C₂₇ are closely correlated with that of the $\delta^{13}\text{C}$ of bulk organic matter and the $\delta^{13}\text{C}$ of all other n -alkane homologs (Table 2). So, the primary sources of organic matter in the sediments of Youganwo Formation were mainly composed of aquatic algae and macrophytes, including some of the aquatic (or terrestrial) higher plants input. Since the $\delta^{13}\text{C}_{\text{org}}$ are highly correlated with the $\delta^{13}\text{C}$ of n -alkanes (Table 2), the $\delta^{13}\text{C}$ variation of medium and high carbon number n -alkanes on the profile is likely not caused by the changes in the source inputs of organic matter, but possibly correlated with the variation of atmospheric $p\text{CO}_2$ during the late Paleocene. In addition, the $\delta^{13}\text{C}$ of all individual n -alkane compounds on the profile display a positive excursion trend from the bottom to the top, and the $\delta^{13}\text{C}$ of the n -alkanes display dramatic changes in the section II of the profile (Figure 7). The general upward positive excursion and the dramatic changes of the $\delta^{13}\text{C}$ of n -alkanes on the profile may correlate with the general decline trend and with the frequent fluctuations in the atmospheric $p\text{CO}_2$ during the late Paleocene (McKay et al., 2016).

Among the steranes, only C₃₀-4-methyl steranes are present in high abundance in all samples of the whole profile. The C₃₀-4-methyl steranes are considered as derived from *Dinoflagellates*

or methylotrophic bacteria. The methylotrophic bacteria prefer to consume isotopically lighter methane generated from the methanogens and would consequently result in isotopically lighter lipids (biomarkers) (Games et al., 1978), while the $\delta^{13}\text{C}$ composition of C₃₀-4-methyl steranes are in the range of -11.93 to -6.28‰ (Table 3) which are very heavier. Therefore, the high abundance of C₃₀-4-methyl steranes was most likely derived from *Dinoflagellates* due to its much heavier $\delta^{13}\text{C}$ composition.

TABLE 3 | The $\delta^{13}\text{C}$ of source-specific compounds of C₃₀-4-methyl sterane, C₃₁-Botryococcane, and C₃₃-Botryococcane in some representative samples.

Sample name	Borehole depth (m)	$\delta^{13}\text{C}_{\text{C}30-4\text{-mest}}$ (‰)	$\delta^{13}\text{C}_{\text{B-C}31}$ (‰)	$\delta^{13}\text{C}_{\text{B-C}33}$ (‰)
MY-3	815	-10.4	-4.5	-4.6
MY-7	817.8	-9.8	-	-7.2
MY-8	818.4	-11.8	n.d.	n.d.
MY-12	821	n.d.	-7.5	-8.4
MY-17	824.6	-11.4	n.d.	n.d.
MY-22	827.5	-11.9	n.d.	n.d.
MY-35	836.5	-6.3	n.d.	n.d.

$\delta^{13}\text{C}_{\text{C}30-4\text{-mest}}$ for C₃₀-4-methyl sterane; $\delta^{13}\text{C}_{\text{B-C}31}$ for C₃₁-Botryococcane; $\delta^{13}\text{C}_{\text{B-C}33}$ for C₃₃-Botryococcane; "n.d." represents not determined.

Meanwhile, the $\delta^{13}\text{C}$ composition of the botryococcanes is very heavier and ranges from -4.5 to -8.4‰ (Table 3). The exceptional heavier $\delta^{13}\text{C}$ of C_{33} -botryococcanes could not be explained by sedimentary conditions alone. Under an aquatic condition of CO_2 (aq) exhaustion, *B. braunii* had to take alternative carbon source by triggering its bicarbonate (HCO_3^-) consumption mechanism (Cepak and Lukavsky, 1994). Since the partial pressure of atmospheric carbon dioxide ($p\text{CO}_2$) during the late Paleocene was significantly lower (Galeotti et al., 2016; Steinhorsdottir et al., 2016) and this could result in low concentration of dissolved CO_2 (aq) in the lake water, and therefore triggered bicarbonate consumption mechanism of the *B. braunii* (Huang et al., 1999). HCO_3^- assimilation by *B. braunii* would cause a significant heavier $\delta^{13}\text{C}$ composition of organic matter generated by the *B. braunii* and other algae. Hence, the extreme heavy $\delta^{13}\text{C}$ composition of the C_{33} -botryococcanes and the C_{31} -botryococcanes in the samples on the top section of the Youganwo Formation suggests that the atmospheric $p\text{CO}_2$ during the late Paleocene decreased significantly in the low altitude continental region and frequently resulted in lower CO_2 (aq) concentration in lake water and therefore would have triggered bicarbonate consumption mechanism of the *B. braunii*.

According to the previous studies, the atmospheric $p\text{CO}_2$ in the late Paleogene displayed a general decreased trend but associated with sharp fluctuations (Pagani et al., 2005; Pearson et al., 2009; Galeotti et al., 2016). So, a general positive excursion associated with significant fluctuation in the $\delta^{13}\text{C}$ composition of the *n*-alkanes on the profile of Maoming oil shales, especially the frequently and sharply variation in the section II, could be considered as correlated to the atmospheric $p\text{CO}_2$ variation during the late Paleogene, while the heavier $\delta^{13}\text{C}$ composition of some source specific biomarkers would be indication of the lower concentration aquatic CO_2 in the lake water due to the lower atmospheric $p\text{CO}_2$ which caused the bicarbonate consumption mechanism of algae such as *B. braunii*. Therefore, the variation in the $\delta^{13}\text{C}$ composition of the *n*-alkanes on the profile and a general positive excursion from the bottom to the top could be considered as responses to the atmosphere $p\text{CO}_2$ decline and variation toward the late Paleogene.

CONCLUSION

The characteristics of organic matter in the Maoming oil shales of Youganwo Formation suggest that the organic matter were

REFERENCES

- Aichner, B., Herzsuh, U., Wilkes, H., Vieth, A., and Böhner, J. (2010). δD values of *n*-alkanes in Tibetan lake sediments and aquatic macrophytes—A surface sediment study and application to a 16ka record from Lake Koucha. *Organ. Geochem.* 41, 779–790. doi: 10.1016/j.orggeochem.2010.05.010
- Ao, H., Dupont-Nivet, G., Rohling, E. J., Peng Zhang, P., Ladant, J. B., Roberts, A. P., et al. (2020). Orbital climate variability on the northeastern Tibetan Plateau across the Eocene-Oligocene transition. *Nat. Commun.* 11:5249.
- Brassell, S. C., Eglinton, G., and Fu, J. M. (1986). Biological marker compounds as indicators of the depositional history of the Maoming oil shale. *Organ. Geochem.* 10, 927–941. doi: 10.1016/s0146-6380(86)80030-4
- Bureau of Geology and Mineral Resources of Guangdong Province (1996). *Stratigraphy (Lithostratic) of Guangdong Province*. Wuhan: China University of Geosciences Press, 177–178.
- Cepak, V., and Lukavsky, J. (1994). The effect of high irradiances on growth, biosynthetic activities and the ultrastructure of the green alga *Botryococcus braunii* strain Droop 1950/807-1. *Algol. Stud.* 72, 115–131.
- Chow, M. C. (1956). Supplementary notes on *Anosteira maomingensis*. *Acta Palaeontol. Sin.* 4, 233–237.
- mainly derived from the aquatic algae input associated with a small portion of aquatic/terrestrial high plant inputs. The $\delta^{13}\text{C}$ composition of the *n*-alkanes, which varied from -31.7 to -16.2‰ , display a general upward positive excursion but with frequent and significant fluctuation in the section II of the profile may reflect the regional responses of low altitude continent to the climate change during the late Paleogene. The extreme heavy $\delta^{13}\text{C}$ composition of the C_{33} -botryococcanes and C_{31} -botryococcanes and C_{30} -4-methyl steranes in some samples in the section I of the upper profile are ranged from -4.5 to -11.9‰ , which is the results of carbon source shift when the aquatic CO_2 exhaustion caused by the decline in atmospheric $p\text{CO}_2$ triggered the bicarbonate consumption mechanism of algae such as *Botryococcus braunii*. The upward positive excursion trend and variation in the profile of the $\delta^{13}\text{C}$ composition of the individual hydrocarbon compounds in the oil shales of the Youganwo Formation would be obvious evidence for the $p\text{CO}_2$ variation and descent toward the late Paleogene.

DATA AVAILABILITY STATEMENT

The original contributions presented in the study are included in the article/supplementary material, further inquiries can be directed to the corresponding author/s.

AUTHOR CONTRIBUTIONS

XC carried out the field sampling and most of the lab experiments and wrote the draft of this manuscript. ZS organized the project and experimental works and edited and finalized the manuscript. SW and PL carried out some experiments and assisted field sampling and data analysis. All authors contributed to the article and approved the submitted version.

FUNDING

This study was financially supported by the National Science Foundation of China (No. 41773037), the Guangxi Natural Science Foundation (No. 2018GXNSFBFA050049), the Open Fund of Key Laboratory of Environment Change and Resources Use in Beibu Gulf, Ministry of Education (GTEU-KLOP-X1803), and the Research Starting Foundation of Nanning Normal University (0819-2018L01).

- Chow, M. C., and Yeh, H. K. (1962). A new emydoid from the Eocene of Maoming, Kwangtung. *Verteb. Palasiat.* 6, 221–229.
- Colwyn, D. A., and Hren, M. T. (2019). An abrupt decrease in Southern Hemisphere terrestrial temperature during the Eocene-Oligocene transition. *Earth Planet. Sci. Lett.* 512, 227–235. doi: 10.1016/j.epsl.2019.01.052
- Coxall, H. K., Wilson, P. A., Pälike, H., Lear, H. C., and Backman, J. (2005). Rapid stepwise onset of Antarctic glaciation and deeper calcite compensation in the Pacific Ocean. *Nature* 433, 53–57. doi: 10.1038/nature03135
- Damsté, J. S. S., Verschuren, D., Ossebaer, J., Blokker, J., Houten, R. V., Meer, M. T. J., et al. (2011). A 25,000-year record of climate-induced changes in lowland vegetation of eastern equatorial Africa revealed by the stable carbon-isotopic composition of fossil plant leaf waxes. *Earth Planet. Sci. Lett.* 302, 236–246. doi: 10.1016/j.epsl.2010.12.025
- Dupont-Nivet, G., Krijgsman, W., Langereis, C. G., Abels, H. A., Dai, S., and Fang, X. (2007). Tibetan plateau aridification linked to global cooling at the Eocene-Oligocene transition. *Nature* 445, 635–638. doi: 10.1038/nature05516
- Eglinton, G., and Hamilton, R. J. (1967). Leaf epicuticular waxes. *Science* 156, 1322–1334. doi: 10.1126/science.156.3780.1322
- Eldrett, J. S., Greenwood, D. R., Harding, I. C., and Huber, M. (2009). Increased seasonality through the Eocene to oligocene transition in northern high latitudes. *Nature* 459, 969–973. doi: 10.1038/nature08069
- Fang, X. M., Galy, A., Yang, Y. B., Zhang, W. L., Ye, C. C., and Song, C. H. (2019). Paleogene global cooling-induced temperature feedback on chemical weathering, as recorded in the northern Tibetan Plateau. *Geology* 47, 992–996. doi: 10.1130/g46422.1
- Ficken, K. J., Li, B., Swain, D. L., and Eglinton, G. (2000). An n-alkane proxy for the sedimentary input of submerged/floating freshwater aquatic macrophytes. *Organ. Geochem.* 3, 745–749. doi: 10.1016/s0146-6380(00)00081-4
- Fu, J. M., Xu, F. F., Chen, D. Y., Liu, D. H., Hu, C. Y., Jia, R. F., et al. (1985). Biomarker compounds of biological inputs in Maoming oil shale. *Geochemica* 2, 99–114.
- Galeotti, S., DeConto, R., Naish, T., Stocchi, P., Florindo, F., Pagani, M., et al. (2016). Antarctic Ice Sheet variability across the Eocene-Oligocene boundary climate transition. *Science* 352, 76–80. doi: 10.1126/science.aab0669
- Gallagher, S. J., Wade, B., Li, Q. Y., Holdgate, G. R., Bown, P., Korasidis, V. A., et al. (2020). Eocene to Oligocene high paleolatitude neritic record of Oi-1 glaciation in the Otway Basin southeast Australia. *Glob. Planet. Chang.* 191:103218. doi: 10.1016/j.gloplacha.2020.103218
- Games, L. M., HayesRobert, J. M., and Gunsalus, P. (1978). Methane-producing bacteria: natural fractionations of the stable carbon isotopes. *Geochim. Cosmoch. Acta* 42, 1295–1297. doi: 10.1016/0016-7037(78)90123-0
- Gelpi, E., Schneider, H., Mann, J., and Oro, J. (1970). Hydrocarbons of geochemical significance in microscopic algae. *Phytochemistry* 9, 603–612. doi: 10.1016/s0031-9422(00)85700-3
- Goldner, A., Herold, N., and Huber, M. (2014). Antarctic glaciation caused ocean circulation changes at the Eocene-Oligocene transition. *Nature* 511, 574–577. doi: 10.1038/nature13597
- Herman, A. B., Spicer, R. A., Aleksandrova, G. N., Yang, J., Kodrul, T. M., Maslova, N. P., et al. (2017). Eocene-early Oligocene climate and vegetation change in southern China: evidence from the Maoming Basin. *Palaeogeogr. Palaeoclimatol. Palaeoecol.* 479, 126–137. doi: 10.1016/j.palaeo.2017.04.023
- Hren, M. T., Sheldon, N. D., Grimes, S. T., Collinson, M. E., Hooker, J. J., Bugler, M., et al. (2013). Terrestrial cooling in Northern Europe during the Eocene-Oligocene transition. *Proc. Natl. Acad. Sci. U.S.A.* 110, 7562–7567. doi: 10.1073/pnas.1210930110
- Huang, Y. S., Street-Perrott, F. A., Perrot, R. A., Metzger, P., and Eglinton, G. (1999). Glacial-interglacial environmental changes inferred from molecular and compound-specific $\delta^{13}\text{C}$ analyses of sediments from Sacred Lake, Mt. Kenya. *Geochim. Cosmochim. Acta* 63, 1383–1404. doi: 10.1016/s0016-7037(99)00074-5
- Jin, J. H. (2008). On the age of the You-gan-wo Formation in the Maoming Basin, Guangdong province. *J. Stratigr.* 32, 47–50.
- Kristen, I., Wilkes, H., Vieth, A., Zink, K. G., Plessen, B., Thorpe, J., et al. (2010). Biomarker and stable carbon isotope analyses of sedimentary organic matter from Lake Tswaing: evidence for deglacial wetness and early Holocene drought from South Africa. *J. Paleolimnol.* 44, 143–160. doi: 10.1007/s10933-009-9393-9
- Li, Y., Song, Z. G., Cao, X. X., and George, S. C. (2016). Sedimentary organic matter record of early cretaceous environmental changes in western Liaoning Province, NE China. *Organ. Geochem.* 98, 54–65. doi: 10.1016/j.orggeochem.2016.05.010
- Li, Y. X., Jiao, W. J., Liu, Z. H., Jin, J. H., Wang, D. H., He, Y. X., et al. (2016). Terrestrial responses of low-latitude Asia to the Eocene-oligocene climate transition revealed by integrated chronostratigraphy. *Clim. Past* 12, 255–272. doi: 10.5194/cp-12-255-2016
- Liao, J., Lu, H., Feng, Q., Zhou, Y. P., Shi, Q., Peng, P. A., et al. (2018). Two novel decamethylhenicosanes (C31H64) identified in a Maoming Basin shale, China. *Organ. Geochem.* 125, 212–219. doi: 10.1016/j.orggeochem.2018.09.012
- Liu, Z. H., He, Y. X., Jiang, Y. Q., Wang, H. Y., Liu, W. G., Bohaty, S. M., et al. (2018). Transient temperature asymmetry between hemispheres in the Paleogene Atlantic Ocean. *Nat. Geosci.* 11, 656–660. doi: 10.1038/s41561-018-0182-9
- Liu, Z. H., Pagani, M., Zinniker, D. A., Deconto, R., Huber, M., and Brinkhuis, H. (2009). Global cooling during the Eocene-Oligocene climate transition. *Science* 323, 1187–1190. doi: 10.1126/science.1166368
- McKay, D. I. A., Tyrrell, T., and Wilson, P. A. (2016). Global carbon cycle perturbation across the Eocene-Oligocene climate transition. *Paleoceanography* 31, 311–329. doi: 10.1002/2015pa002818
- McKirdy, D. M., Cox, R. E., Volkman, J. K., and Howell, V. J. (1986). Botryococcane in a new class of Australian non-marine crude oils. *Nature* 320, 57–59. doi: 10.1038/320057a0
- Meng, Q. T., Li, J. G., Liu, Z. J., Hu, F., and Xu, C. (2020). Organic geochemical characteristics and depositional environment of oil shale of eocene of paleocene youganwo formation in yangjiao mining area of Maoming Basin. *J. Jilin Univ.* 50, 356–376.
- Meyers, P. A. (2003). Applications of organic geochemistry to paleolimnological reconstructions: a summary of examples from the Laurentian Great Lakes. *Organ. Geochem.* 34, 261–289. doi: 10.1016/s0146-6380(02)00168-7
- Moldovan, J. M., and Seifert, W. K. (1980). First discovery of botryococcane in petroleum. *J. Chem. Soc. Chem. Commun.* 19, 912–914. doi: 10.1039/c39800000912
- Mügler, I., Sachse, D., Werner, M., Xu, B., Wu, G., Yao, T., et al. (2008). Effect of lake evaporation on δD values of lacustrine n-alkanes: a comparison of Nam Co (Tibetan Plateau) and Holzmaar (Germany). *Organ. Geochem.* 39, 711–729. doi: 10.1016/j.orggeochem.2008.02.008
- Pagani, M., Zachos, J. C., Freeman, K. H., Tipler, B., and Bohaty, S. (2005). Marked decline in atmospheric carbon dioxide concentrations during the Paleogene. *Science* 309, 600–603. doi: 10.1126/science.1110063
- Passchier, S., Ciarletta, D. J., Miriagos, T. E., Bijl, P. K., and Bohaty, S. M. (2017). An Antarctic stratigraphic record of stepwise ice growth through the Eocene-Oligocene transition. *Geo. Soc. Am. Bull.* 129, 318–330. doi: 10.1130/b31482.1
- Pearson, P. N., Foster, G. L., and Wade, B. S. (2009). Atmospheric carbon dioxide through the Eocene-Oligocene climate transition. *Nature* 461, 1110–1113. doi: 10.1038/nature08447
- Pei, J. L., Sun, Z. M., Zhao, Y., Wang, X. S., and Li, H. B. (2007). Eocene-Oligocene boundary global cooling event recorded in the Qaidam Basin, Qinghai, China. *Geol. Bull. China* 26, 1380–1384.
- Peters, K. E., and Cassa, M. R. (1994). “Applied source rock geochemistry,” in *The Petroleum System-From Source to Trap*, eds L. B. Magoon and W. G. Dow (Oklahoma: The American Association of petroleum Geologists Tulsa), 93–120. doi: 10.1306/m60585c5
- Smittenberg, R. H., Baas, M., Schouten, S., and Damsté, J. S. S. (2005). The demise of the alga *Botryococcus braunii* from a Norwegian fjord was due to early eutrophication. *Holocene* 15, 133–140. doi: 10.1191/0959683605hl786rp
- Steinhorsdottir, M., Porter, A. S., Holohan, A., Kunzmann, L., Collinson, M., and McElwain, J. C. (2016). Fossil plant stomata indicate decreasing atmospheric CO_2 prior to the Eocene - Oligocene boundary. *Clim. Past* 12, 439–454. doi: 10.5194/cp-12-439-2016
- Stephen, T. G., Hooker, J. J., Collinson, M. E., and Matthey, D. P. (2005). Summer temperatures of late Eocene to early Oligocene freshwaters. *Geology* 33, 189–192. doi: 10.1130/g21019.1
- Tripathi, A., Backman, J., Elderfield, H., and Ferretti, P. (2005). Eocene bipolar glaciation associated with global carbon cycle changes. *Nature* 436, 341–346. doi: 10.1038/nature03874

- Volkman, J. K. (2014). Acyclic isoprenoid biomarkers and evolution of biosynthetic pathways in green microalgae of the genus *Botryococcus*. *Organ. Geochem.* 75, 36–47. doi: 10.1016/j.orggeochem.2014.06.005
- Yu, J. F., and Wu, Z. J. (1983). Sporopollen assemblage of Mao 5 well of Maoming Basin, Guangdong and its geological age. *J. Stratigr.* 7, 112–118.
- Yu, Z. Q., Peng, P. A., Sheng, G. Y., and Fu, J. M. (2000). Biomarker carbon isotopic components of Tertiary oil shales in Maoming and Jiangnan Basin. *Sci. Bull.* 45(Suppl.), 2783–2789.
- Zhou, Y. P., Shi, J. Y., Xiang, M. J., and Qu, D. C. (1998). Origin study of geohopanes from different depositional environments-stable carbon isotopic evidences. *Acta Sedimentol. Sin.* 16, 14–19.

Conflict of Interest: The authors declare that the research was conducted in the absence of any commercial or financial relationships that could be construed as a potential conflict of interest.

Copyright © 2021 Cao, Song, Wang and Lyu. This is an open-access article distributed under the terms of the Creative Commons Attribution License (CC BY). The use, distribution or reproduction in other forums is permitted, provided the original author(s) and the copyright owner(s) are credited and that the original publication in this journal is cited, in accordance with accepted academic practice. No use, distribution or reproduction is permitted which does not comply with these terms.